Coordination Chemistry

DOI: 10.1002/anie.201410828

Synthesis and Platinum Complexes of an Alane-Appended 1,1′-Bis(phosphino)ferrocene Ligand**

*Bradley E. Cowie, Fu An Tsao, and David J. H. Emslie**

Abstract: *An aryldimethylalane-appended analogue of 1,1′-bis(diphenylphosphino)ferrocene, FcPPAl, was prepared, and reaction with [Pt(nb)$_3$] (nb = norbornene) afforded [Pt(η^2-nb)(FcPPAl)] (**1**). Heating a solution of **1** to 80 °C resulted in crystallization of [{Pt(FcPPAl)}$_2$] (**2**), whereas treatment of **1** with C_2H_4, C_2Ph_2, H_2, or CO provided [PtL(FcPPAl)] [L = C_2H_4 (**3**), C_2Ph_2 (**4**)], [PtH$_2$(FcPPAl)] (**5**), and [Pt(CO)(FcPPAl)] (**6**). In all complexes, the FcPPAl ligand is coordinated through both phosphines and the alane. Whereas **2** adopts a T-shaped geometry at platinum, **3**–**5** are square-pyramidal, and **6** is distorted square-planar. The hydride and carbonyl complexes feature unusual multicenter bonding involving platinum, aluminum, and a hydride or carbonyl ligand.*

Transition metal complexes bearing σ-acceptor ligands (Z-type ligands) have enjoyed a renaissance in the last decade, and are of interest given the ability of Z-type ligands to reduce the number of d-electrons in the frontier orbitals by two units without changing the overall electron count, to elicit unusual metal geometries,[1] to modulate the amount of electron density at the metal center in different oxidation states,[2] to exert a high *trans* influence, and to interact with substrates and co-ligands.[3] Within this area, the vast majority of the research has focused on borane Lewis acids,[4] and has relied upon ambiphilic ligands to stabilize metal–borane interactions, since unsupported metal–borane compounds have thus far evaded isolation.

The situation changes upon moving down Group 13, where [Cp(CO)$_2$Fe(AlPh$_3$)]$^-$, featuring an unsupported iron–alane bond, was described by Burlitch in 1979,[5] [Cp*(Me$_3$P)IrH$_2$(AlPh$_3$)] was reported in 1998 by Bergman and Andersen,[6] and a series of rhodium and platinum AlX$_3$ (X = Cl, Br, and I) complexes was recently prepared by Braunschweig et al.[7–9] However, only a handful of alane-containing ambiphilic ligands have been reported (Figure 1), and in contrast to the chemistry of borane-containing ambiphilic ligands, most of these ligands have not yielded complexes featuring metal–alane coordination. This is the case for ligands **L1**–**L5** in Figure 1, which engaged in halide or alkyl coordination and abstraction reactions,[10,11] neutral ligand (NEt$_3$ and DMSO) abstraction reactions,[10,12] and acyl or formyl ligand (formed through 1,1-insertion) coordination to form η^2*CO*-coordinated five-membered CR-O-AlR$_2$-N*t*Bu-PR$_2$ rings in preference to metal–alane bonding.[13] However, Lu and co-workers recently developed the alumatrane-containing **L6** ligand, and reported the synthesis of Ni, Fe, and Co complexes featuring κ^4*PPPAl*-coordination; these are the first examples of κ^1*Al*-coordination to a metal by an alane within an ambiphilic ligand framework.[14] Ligand **L7**, which was generated in situ through the reaction of [(Ph$_2$PCH$_2$SiMe$_2$)$_2$N]Ir=C=CH$_2$] with AlMe$_3$ to form [(**L7**)Ir-(CMe=CH$_2$)], was also shown to engage in iridium–aluminum bonding, but in this case, the metal is η^2-bound to nitrogen and aluminum, in addition to both phosphines.[15,16]

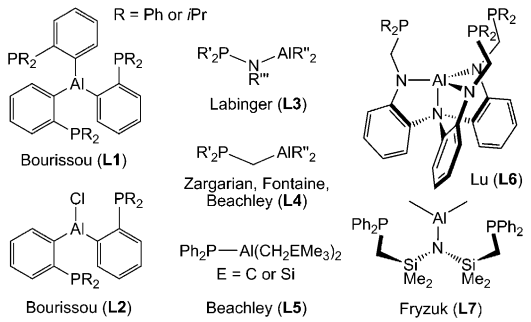

Figure 1. Previously reported alane-containing ambiphilic ligands.

We have previously utilized a rigid phosphine–thioether–borane ligand, TXPB, to investigate the behavior of a pendant borane in the coordination sphere of late transition metals bearing a variety of co-ligands.[17] However, the Achilles heel of the TXPB ligand is the central thioether donor, which readily dissociates from the metal center. In response, a much more electron-donating borane-containing ambiphilic ligand, [Fe(η^5-C$_5$H$_4$PPh$_2$){η^5-C$_5$H$_4$P*t*Bu(C$_6$H$_4$(BPh$_2$)-*o*)}] (FcPPB; a borane-appended analogue of 1,1′-bis(diphenylphosphino)-ferrocene (dppf)), was prepared and complexed with platinum, yielding rare examples of η^3*BCC*-, η^2*BC*-, η^1*B*-coordination and Pt-H-BR$_3$ bridging.[18] Given the small number of known κ^1*Al*-coordinated alane complexes, we sought to prepare an alane-containing analogue of FcPPB. This ligand, [Fe(η^5-C$_5$H$_4$PPh$_2$){η^5-C$_5$H$_4$P*t*Bu(C$_6$H$_4$(AlMe$_2$)-*o*)}] (FcPPAl; Scheme 1), features an AlMe$_2$ group in place of a BPh$_2$ group, and herein we present the first unambiguous examples of κ^1*Al*-coordinated alkylalane complexes.[19]

The FcPPAl ligand was prepared by lithiation of [Fe(η^5-C$_5$H$_4$PPh$_2$){η^5-C$_5$H$_4$P*t*Bu(C$_6$H$_4$Br-*o*)}] (synthesized in six steps

[*] B. E. Cowie, F.-A. Tsao, Prof. D. J. H. Emslie
Department of Chemistry and Chemical Biology
McMaster University
1280 Main St. West, Hamilton, Ontario, L8S 4M1 (Canada)
E-mail: emslied@mcmaster.ca

[**] D.J.H.E. thanks NSERC of Canada for a Discovery Grant and B.E.C. thanks the Government of Canada for an NSERC PGS-D scholarship. We are grateful to J. S. Price for PXRD experiments.

Supporting information for this article is available on the WWW under http://dx.doi.org/10.1002/anie.201410828.

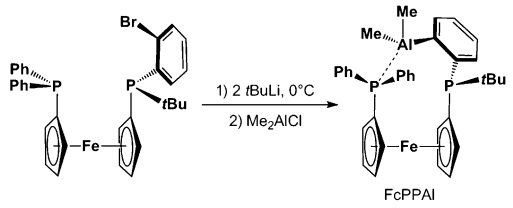

Scheme 1. Synthesis of the FcPPAl ligand.

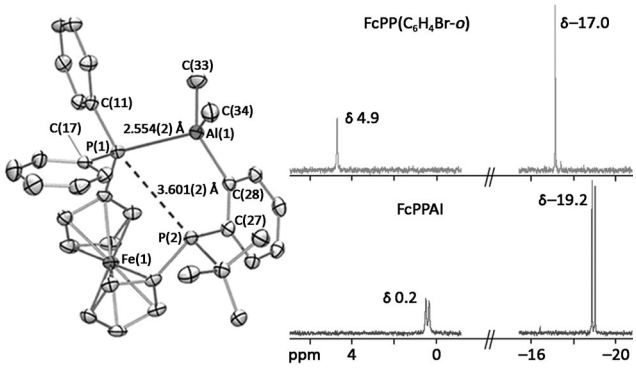

Figure 2. Solid-state structure of FcPPAl (left) with ellipsoids drawn at 50% probability. The dotted line highlights the spatial relationship between P(1) and P(2); it does not represent a net chemical bond. Hydrogen atoms have been omitted for clarity. Stacked $^{31}P\{^1H\}$ NMR spectra of [Fe(η^5-$C_5H_4PPh_2$){η^5-$C_5H_4PtBu(C_6H_4Br$-*o*)}] (right, top) and FcPPAl (right, bottom).

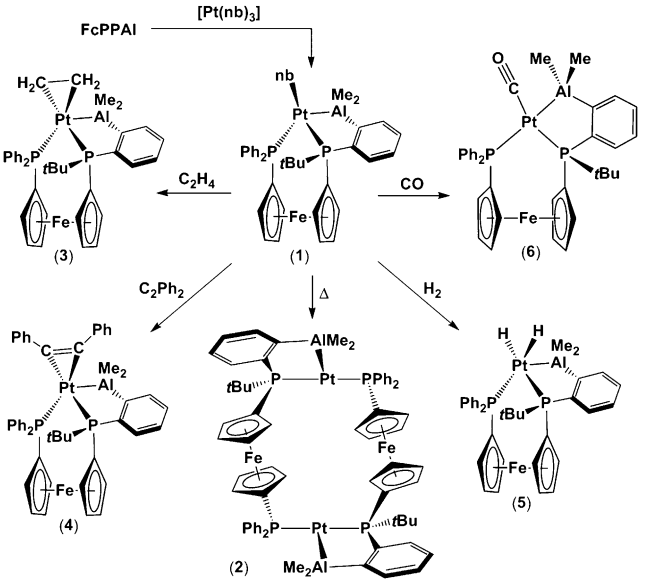

Scheme 2. Synthesis of complexes **1**–**6**.

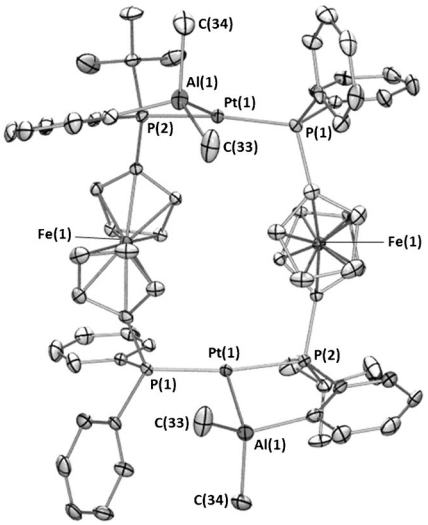

Figure 3. Solid-state structure of **2** with ellipsoids drawn at 50% probability. Hydrogen atoms have been omitted for clarity.

from $FeCp_2$ and $C_6H_4Br_2$-*o*)[18] and quenching with Me_2AlCl (Scheme 1). FcPPAl is chiral at phosphorus, and was used as a racemic mixture. In the solid state, P(1) is engaged in adduct formation with the alane (Figure 2; P(1)–Al = 2.554(2) Å), whereas recently reported FcPPB features a P(2)–B interaction;[18] presumably a P(1)–B interaction is disfavored by the *B*-phenyl substituents in FcPPB. In the ^{31}P NMR spectrum of FcPPAl, a ^{31}P–^{31}P coupling of 31 Hz (Figure 2) is indicative of through-space coupling arising from a nonbonding interaction between the lone pair on P(2) and the bonding pair between P(1) and Al;[20] the P(1)–P(2) distance in FcPPAl is 3.601(2) Å.

Reaction of FcPPAl with $[Pt(nb)_3]$ (nb = norbornene) afforded [Pt(η^2-nb)(FcPPAl)] (**1**) in which platinum is coordinated to both phosphines and one equivalent of norbornene, based on ^1H, ^{13}C, ^{31}P, and ^{195}Pt NMR data. Two sharp AlMe_2 signals were observed in the ^1H NMR spectrum of **1**, indicating that the alane is also bound to platinum. In toluene at 80 °C, **1** dissociates norbornene and dimerizes to afford [{Pt(FcPPAl)}$_2$] (**2**), which crystallizes from solution (Scheme 2). Despite the insolubility of complex **2**, during the course of the reaction, unreacted **1** and trace amounts of **2** may be observed by $^{31}P\{^1H\}$ NMR spectroscopy, giving rise to a large ^{31}P–^{31}P coupling (356 Hz) indicative of *trans*-disposed phosphines. An X-ray crystal structure of **2**, which is formed as the *rac* diastereomer, revealed that each FcPPAl ligand is κ^2*PAl*-coordinated to one platinum center and κ^1*P*-coordinated to the other (Figure 3; powder X-ray diffraction (PXRD) confirmed that the bulk sample of **2** consists only of the *rac* diastereomer). Both platinum centers are equivalent with a distorted T-shaped geometry and *trans* phosphine ligands. The Pt–Al distance in **2** is 2.482(1) Å, and the alane is substantially pyramidalized, with the sum of the C-Al-C angles equal to 336.7(3)°. The geometry of **2** stands in stark contrast to that of [Pt(FcPPB)], which is pseudo square-planar with η^3*BCC*-coordination of the arylborane.[18]

Reaction of **1** with ethylene or diphenylacetylene afforded [Pt(η^2-C_2H_4)(FcPPAl)] (**3**) and [Pt(η^2-C_2Ph_2)(FcPPAl)] (**4**) (Scheme 2) with Pt–Al distances of 2.533(4) and 2.570(2) Å, respectively (Figure 4; Σ(C-Al-C) = 333(1) and 334.0(5)°). The C(35)–C(36) distances are 1.40(2) in **3** and 1.291(8) Å in **4**, and the C–C stretching frequencies are 1156 and 1735 cm^{-1}, respectively, indicative of metallacyclopropane and metallacyclopropene complexes. The coordination geometry of **3** and

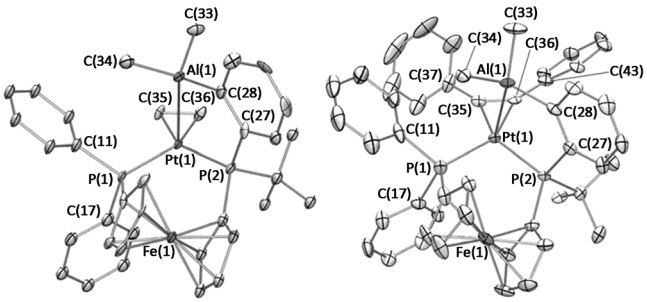

Figure 4. Solid-state structures of **3** (left) and **4** (right) with ellipsoids drawn at 50% probability. Hydrogen atoms have been omitted for clarity.

4 is therefore best described as distorted square-pyramidal, with Al(1) occupying the apical position. The reactivity of "Pt(FcPPAl)" with alkenes and alkynes is distinct from that of [Pt(FcPPB)], which does not react with norbornene, C_2H_4, or C_2Ph_2.[18]

The dihydride complex, [PtH_2(FcPPAl)] (**5**), was prepared through reaction of **1** with H_2 (Scheme 2), and whereas [PtH_2(FcPPB)] reverts back to [Pt(FcPPB)] and H_2 at room temperature in vacuo in the solid state, or in solution under argon,[18] **5** is stable in vacuo, and at 75 °C in solution. The thermal stability of **5** is also notable in light of the reactivity of [Cp*$IrH_2(PMe_3)$] with $AlPh_3$ and $AlEt_3$; the former reaction provided stable [Cp*$(Me_3P)IrH_2(AlPh_3)$], whereas in the latter reaction, the weaker Al–C bonds in $AlEt_3$ resulted in ethane elimination to form [{Cp*$(PMe_3)Ir(\mu\text{-}AlEt)\}_2$].[6] No ^1H–^1H coupling was observed between the hydride signals in **5**, and Pt–H stretches were observed at 2101 and 2049 cm^{-1} in the IR spectrum (nujol mull). The FcPPAl ligand in **5** is κ^3*PPAl*-coordinated, resulting in a distorted square-pyramidal geometry at platinum with the alane in the apical position (Figure 5; Pt–Al = 2.5105(7) Å; Σ(C-Al-C) = 337.0(2)°).

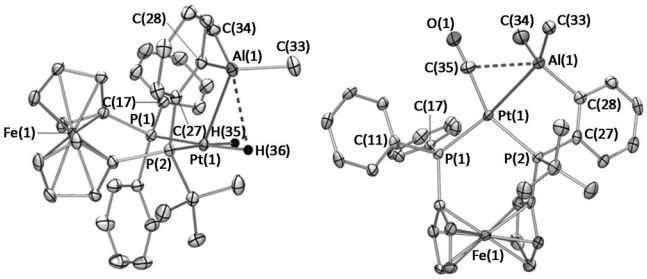

Figure 5. Solid-state structures of **5** (left) and **6** (right) with ellipsoids drawn at 50% probability. Most hydrogen atoms have been omitted for clarity.

Notably, the Al–H(36) and Al–H(35) distances are 2.46(4) and 2.86(3) Å, respectively, and the Al-Pt-H(36) bond angle is 69(1), versus 86(1)° for Al-Pt-H(35), suggestive of a bonding interaction between the alane and H(36). For comparison, the DFT-calculated structure for [PtH_2(FcPPB)] is square-planar with a short interaction between the borane and one of the hydride ligands (B–H = 1.386 Å; Pt–B = 2.524 Å).[18]

Reaction of **1** with CO afforded [Pt(CO)(FcPPAl)] (**6**; Scheme 2) with a Pt–Al distance of 2.624(2) Å (Σ(C-Al-C) = 337.9(5)°; Figure 5), and a CO stretch at 1982 cm^{-1} (nujol mull). Platinum is distorted square-planar with CO located approximately in the P(1)-Pt-P(2) plane, and Al located 1.05 Å out of the plane, leading to a P(1)-Pt-Al angle of 155.38(5)°. The Al-Pt-CO angle in **6** is extremely acute (73.0(2)°), placing CO just 2.736(8) Å from Al, hinting at a bonding interaction between the alane and the CO co-ligand. The bonding situation in **2** differs from that in [Pt(CO)(FcPPB)], which is distorted tetrahedal with η^2*BC*-coordination of the arylborane to platinum.[18]

The Pt–Al distances in **2**–**6** range from 2.482(1) to 2.624(2) Å, increasing in the order **2** < **5** < **3** < **4** < **6**. The Pt–Al distances in [$Pt(PR_3)L(AlX_3)$] (L = PR_3, NHC; X = Cl, Br)[8,9] are considerably shorter than those in **2**–**6**, ranging from 2.37 to 2.39 Å, likely due to the greater Lewis acidity of AlX_3 relative to a dialkylarylalane. However, after adjusting for differences in covalent radius,[21] the M–Al distances in Lu's diamagnetic [Ni(**L6**)] (Ni–Al = 2.450(1) Å) and paramagnetic [$Fe(N_2)$(**L6**)] (Fe–Al = 2.809(2) Å) complexes are comparable with those in **2**–**6**.[14]

DFT calculations (ADF, gas phase, PBE, D3-BJ, all-electron, TZ2P, ZORA) on **3**–**6** afforded geometries ($\mathbf{3}_{calc}$–$\mathbf{6}_{calc}$) in good agreement with the X-ray crystal structures. The Pt–Al Nalewajski–Mrozek (NM; Set 3)[22] bond orders in $\mathbf{3}_{calc}$–$\mathbf{6}_{calc}$ are 0.39, 0.37, 0.37, and 0.34, respectively (cf. 0.40–0.46 for the Pt–P bonds), indicative of significant Pt–Al bonding. The Al–H(36) and Al–C(35) NM bond orders in $\mathbf{5}_{calc}$ and $\mathbf{6}_{calc}$ are 0.12 and 0.18, respectively, suggesting an interaction between the alane and an adjacent H or CO ligand, consistent with the acute Al-Pt-H(36) and Al-Pt-C(35) angles (calcd. 72° and 73°, respectively).

For each structure, several MOs exhibit Pt–Al bonding character, but the bonding picture is complicated by the highly delocalized nature of the MOs. Consequently, the structures of model [$PtH_2(PMe_3)_2(AlMe_2Ph)$] ($\mathbf{5}_{calc}'$) and [$Pt(CO)(PMe_3)_2(AlMe_2Ph)$] ($\mathbf{6}_{calc}'$) were geometry optimized, constraining the Pt, P, Al, C_{CO} and hydride positions to be identical to those in $\mathbf{5}_{calc}$ and $\mathbf{6}_{calc}$. The Pt–Al NM bond orders for $\mathbf{5}_{calc}'$ and $\mathbf{6}_{calc}'$ are 0.38 and 0.34, respectively, the Al–H(36) NM bond order in $\mathbf{5}_{calc}'$ is 0.12, and the Al–C(35) bond order in $\mathbf{6}_{calc}'$ is 0.18. The bonding situation in $\mathbf{5}_{calc}'$ and $\mathbf{6}_{calc}'$ was further examined using natural bond order (NBO) and natural localized molecular orbital (NLMO) analysis.

For $\mathbf{5}_{calc}'$, two NLMOs participate significantly in Pt–Al and Al–H bonding; *a* in Figure 6 contributes 0.10 to the total Pt–Al NLMO bond order of 0.33, and *b* contributes 0.12 to both the Pt–Al and Al–H bond orders (the total Al–H NLMO bond order in $\mathbf{5}_{calc}'$ is 0.12). In compound $\mathbf{6}_{calc}'$, NLMOs d–f in Figure 6 contribute 0.18, 0.06, and 0.13, respectively to the total Pt–Al NLMO bond order of 0.31, and NLMOs d and f contribute 0.12 and 0.13 to the total Al–C(35) bond order of 0.25. These NLMOs highlight the presence of an unusual multicenter bonding situation involving Pt, Al, and the carbonyl carbon atom; effectively, the electrons involved in σ-donation and π-backdonation between C(35) and Pt are also involved in bonding to Al. SCF deformation density isosurfaces for $\mathbf{5}_{calc}'$ and $\mathbf{6}_{calc}'$ in Figure 6 illustrate

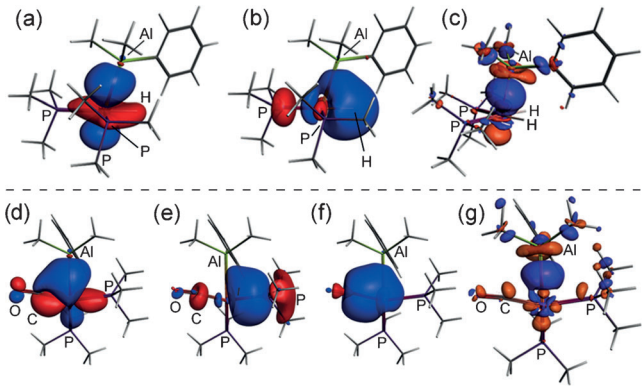

Figure 6. a,b) NLMOs for $\mathbf{5}_{calc}'$, d–f) NLMOs for $\mathbf{6}_{calc}'$, and (c and g) SCF deformation density (SCFDD) isosurfaces from fragment analysis of $\mathbf{5}_{calc}'$ and $\mathbf{6}_{calc}'$, respectively; purple and orange indicate regions of increased and depleted electron density, respectively. In all cases, platinum is the central atom. Isosurfaces are set to 0.03 for NLMOs, and 0.003 in the SCFDD plots.

regions of increased and decreased electron density upon $(PMe_3)_2L_xPt$ and $AlMe_2Ph$ fragment combination.

In conclusion, an aryldimethylalane-appended analogue of dppf, FcPPAl, has been prepared and employed for the synthesis of the first well-authenticated κ^1*Al*-coordinated alkylalane complexes; **1**–**6**.[19] The geometry at platinum in **1**–**6** is T-shaped, square-pyramidal, or distorted square-planar, and **5** and **6** feature acute Al-Pt-H and Al-Pt-CO angles ($\approx 70°$) due to multicenter bonding involving Al, Pt, and an H or CO ligand. Alane-coordination is rigorously maintained in **1**–**6**, despite variations in the geometry and oxidation state of platinum, and Al–C bond cleavage reactivity was not observed. Differences in the coordination behavior of FcPPAl and FcPPB[18] are reflected in the very different structures and geometries of **2**, **5**, and **6**, relative to FcPPB analogues, the stability of **5** toward H_2 reductive elimination, and the favorability of alkene and alkyne coordination to "Pt(FcPPAl)". This comparison highlights the extent to which the behavior of ambiphilic ligands depends on the precise identity of the Lewis acid.

Experimental Section

Full experimental and characterization details for FcPPAl and **1**–**6**, the details of DFT calculations, NMR spectra of FcPPAl and **1**–**6**, and a powder X-ray diffractogram for **2** are included in the Supporting Information. CCDC 1030593 (FcPPAl), CCDC 1030594 (**2**), CCDC 1030595 (**3**), CCDC 1030596 (**4**), CCDC 1030597 (**5**), CCDC 1030598 (**6**), contain the supplementary crystallographic data for this paper. These data can be obtained free of charge from The Cambridge Crystallographic Data Centre via www.ccdc.cam.ac.uk/data_request/cif.

Received: November 6, 2014
Published online: December 23, 2014

Keywords: alanes · coordination chemistry · donor–acceptor systems · ligand design · platinum

[1] a) G. Parkin, *Organometallics* **2006**, *25*, 4744–4747; b) M. Sircoglou, S. Bontemps, M. Mercy, N. Saffon, M. Takahashi, G. Bouhadir, L. Maron, D. Bourissou, *Angew. Chem. Int. Ed.* **2007**, *46*, 8583–8586; *Angew. Chem.* **2007**, *119*, 8737–8740.
[2] a) A. Amgoune, D. Bourissou, *Chem. Commun.* **2011**, *47*, 859–871; b) M.-E. Moret, J. C. Peters, *Angew. Chem. Int. Ed.* **2011**, *50*, 2063–2067; *Angew. Chem.* **2011**, *123*, 2111–2115.
[3] a) W. H. Harman, T.-P. Lin, J. C. Peters, *Angew. Chem. Int. Ed.* **2014**, *53*, 1081–1086; *Angew. Chem.* **2014**, *126*, 1099–1104; b) T.-P. Lin, R. C. Nelson, T. Wu, J. T. Miller, F. P. Gabbaï, *Chem. Sci.* **2012**, *3*, 1128–1136.
[4] a) A. Amgoune, G. Bouhadir, D. Bourissou, *Top. Curr. Chem.* **2013**, *334*, 281–312; b) G. Bouhadir, A. Amgoune, D. Bourissou, *Adv. Organomet. Chem.* **2010**, *58*, 1–107, and references therein.
[5] J. M. Burlitch, M. E. Leonowicz, R. B. Petersen, R. E. Hughes, *Inorg. Chem.* **1979**, *18*, 1097–1105.
[6] J. T. Golden, T. H. Peterson, P. L. Holland, R. G. Bergman, R. A. Andersen, *J. Am. Chem. Soc.* **1998**, *120*, 223–224.
[7] a) J. Bauer, H. Braunschweig, P. Brenner, K. Kraft, K. Radacki, K. Schwab, *Chem. Eur. J.* **2010**, *16*, 11985–11992; b) J. Bauer, H. Braunschweig, A. Damme, K. Gruß, K. Radacki, *Chem. Commun.* **2011**, *47*, 12783–12785; c) J. Bauer, H. Braunschweig, K. Radacki, *Chem. Commun.* **2012**, *48*, 10407–10409.
[8] J. Bauer, R. Bertermann, H. Braunschweig, K. Gruss, F. Hupp, T. Kramer, *Inorg. Chem.* **2012**, *51*, 5617–5626.
[9] H. Braunschweig, K. Gruss, K. Radacki, *Angew. Chem. Int. Ed.* **2007**, *46*, 7782–7784; *Angew. Chem.* **2007**, *119*, 7929–7931.
[10] a) M.-H. Thibault, J. Boudreau, S. Mathiotte, F. Drouin, O. Sigouin, A. Michaud, F.-G. Fontaine, *Organometallics* **2007**, *26*, 3807–3815; b) J. Boudreau, F.-G. Fontaine, *Organometallics* **2011**, *30*, 511–519.
[11] a) M. Sircoglou, G. Bouhadir, N. Saffon, K. Miqueu, D. Bourissou, *Organometallics* **2008**, *27*, 1675–1678; b) M. Sircoglou, N. Saffon, K. Miqueu, G. Bouhadir, D. Bourissou, *Organometallics* **2013**, *32*, 6780–6784; c) M. Devillard, E. Nicolas, C. Appelt, J. Backs, S. Mallet-Ladeira, G. Bouhadir, J. C. Slootweg, W. Uhl, D. Bourisou, *Chem. Commun.* **2014**, *50*, 14805–14808; d) F.-G. Fontaine, D. Zargarian, *J. Am. Chem. Soc.* **2004**, *126*, 8786–8794.
[12] O. T. Beachley, Jr., M. A. Banks, J. P. Kopasz, R. D. Rogers, *Organometallics* **1996**, *15*, 5170–5174.
[13] a) J. A. Labinger, J. S. Miller, *J. Am. Chem. Soc.* **1982**, *104*, 6856–6858; b) D. L. Grimmett, J. A. Labinger, J. N. Bonfiglio, S. T. Masuo, E. Shearin, J. S. Miller, *J. Am. Chem. Soc.* **1982**, *104*, 6858–6859; c) J. A. Labinger, J. N. Bonfiglio, D. L. Grimmett, S. T. Masuo, E. Shearin, J. S. Miller, *Organometallics* **1983**, *2*, 733–740; d) D. L. Grimmett, J. A. Labinger, J. N. Bonfiglio, S. T. Masuo, E. Shearin, J. S. Miller, *Organometallics* **1983**, *2*, 1325–1332.
[14] a) P. A. Rudd, S. Liu, L. Gagliardi, V. G. Young, Jr., C. C. Lu, *J. Am. Chem. Soc.* **2011**, *133*, 20724–20727; b) P. A. Rudd, N. Planas, E. Bill, L. Gagliardi, C. C. Lu, *Eur. J. Inorg. Chem.* **2013**, 3898–3906.
[15] M. D. Fryzuk, N. T. McManus, S. J. Rettig, G. S. White, *Angew. Chem. Int. Ed. Engl.* **1990**, *29*, 73–75; *Angew. Chem.* **1990**, *102*, 67–68.
[16] M. D. Fryzuk, L. Huang, N. T. McManus, P. Paglia, S. J. Rettig, G. S. White, *Organometallics* **1992**, *11*, 2979–2990.
[17] a) D. J. H. Emslie, J. M. Blackwell, J. F. Britten, L. E. Harrington, *Organometallics* **2006**, *25*, 2412–2414; b) S. R. Oakley, K. D. Parker, D. J. H. Emslie, I. Vargas-Baca, C. M. Robertson, L. E. Harrington, J. F. Britten, *Organometallics* **2006**, *25*, 5835–5838; c) D. J. H. Emslie, L. E. Harrington, H. A. Jenkins, C. M. Robertson, J. F. Britten, *Organometallics* **2008**, *27*, 5317–5325; d) B. E. Cowie, D. J. H. Emslie, H. A. Jenkins, J. F. Britten, *Inorg. Chem.* **2010**, *49*, 4060–4072; e) D. J. H. Emslie, B. E.

Cowie, S. R. Oakley, N. L. Huk, H. A. Jenkins, L. E. Harrington, J. F. Britten, *Dalton Trans.* **2012**, *41*, 3523 – 3535; f) B. E. Cowie, D. J. H. Emslie, *Organometallics* **2013**, *32*, 7297 – 7305.

[18] B. E. Cowie, D. J. H. Emslie, *Chem. Eur. J.* **2014**, *20*, 16899 – 16912.

[19] Several $[CpML_2(AlMe_3)]$ (M = Rh or Co; L = PR_3 or C_2H_4) complexes have been reported; however, none of these complexes were structurally authenticated: see J. M. Mayer, J. C. Calabrese, *Organometallics* **1984**, *3*, 1292 – 1298.

[20] J.-C. Hierso, *Chem. Rev.* **2014**, *114*, 4838 – 4867.

[21] B. Cordero, V. Gómez, A. E. Platero-Prats, M. Revés, J. Echeverría, E. Cremades, F. Barragán, S. Alvarez, *Dalton Trans.* **2008**, 2832 – 2838.

[22] A. Michalak, R. L. DeKock, T. Ziegler, *J. Phys. Chem. A* **2008**, *112*, 7256 – 7263.

